Coupled simulations of radiative transfer and nonequilibrium flow in high altitude rocket plumes

Guillaume Janodet, Jean-Michel Lamet, Philippe Rivière, Valérie Rialland, Anouar Soufiani

COUPLED SIMULATIONS OF RADIATIVE TRANSFER AND NONEQUILIBRIUM FLOW IN HIGH ALTITUDE ROCKET PLUMES

Guillaume Janodet[1,2*], Jean-Michel Lamet[2], Philippe Rivière[1], Valérie Rialland[3], Anouar Soufiani[1]

[1]Laboratoire EM2C, CNRS, CentraleSupélec, Université Paris Saclay, 91192 Gif-sur-Yvette, France
[2]ONERA/DMPE, Université de Toulouse, F-31055, Toulouse, France
[3]ONERA/DOTA, Université Paris-Saclay, BP80100, 91123 Palaiseau Cedex, France

ABSTRACT.

While IR radiation from high altitude rocket plumes is generally computed by post-processing of flow field calculations, this paper presents some models suitable for the full coupling between nonequilibrium radiation and flow field calculations in the framework of multi-temperature description of the thermodynamic state of the medium. Detailed kinetic vibrational models, nonequilibrium statistical narrow-band models implemented in a radiation Monte Carlo solver, and flow field and energy solvers with various vibrational temperatures are coupled and applied to the test case Titan IIIC rocket flying at an altitude of 110 km. The results show that radiative transfer has an important effect on vibrational temperatures, which, in turn, affects radiation level. Self-absorption in the plume is shown to be important and reduces the decrease in vibration temperatures due to radiative losses. In the considered CO_2/H_2O/CO mixtures, the total radiation losses are shown to be mainly due to the vibrational exchanges in the ν_3 mode of CO_2.

1. INTRODUCTION

The prediction of radiative transfer in high altitude rocket plumes has been the subject of several experimental and numerical studies due to its significance for heat transfer to the rocket nozzle and to plume infrared signature (see e.g. [1]). One of the challenging issues in predicting such radiative transfer is the nonequilibrium of the internal energy levels of the medium due to fast flow expansion and a possible freeze of vibrational populations. To the best of our knowledge, there is a lack of detailed studies on the effects of radiation on the plume itself and the temperature fields. As collisions become rare at low pressure, radiative de-excitation and absorption may play an important role in the distribution of level populations, determining radiation transport. Local populations of each rovibrational level can be determined from a vibrational kinetic model associated with either a detailed state-to-state model or a multi-temperature model (see e.g. [2]). Binauld et al. have developed a vibrational kinetic model and line-by-line non-local thermodynamic equilibrium (NLTE) model to predict radiation escaping from high altitude rocket plumes [3]. They selected a few lines of sight and showed that the freezing of CO_2 vibration modes may increase significantly plume signature. In order to enable practicable computations of nonequilibrium radiation coupled to flow field calculations, Janodet et al. [4] have developed and validated a statistical narrow-band model for CO_2 in the framework of a multi-temperature thermodynamic model. The present paper aims to

*Corresponding author: guillaume.janodet@onera.fr

extend this model to gaseous mixtures of practical interest (CO2-H_2O-CO-HCl) and implement it in a Monte Carlo radiation solver. Then, the model is coupled to a flow field multi-temperature solver to investigate radiative transfer effects on vibration temperature fields and plume signature.

2. NONEQUILIBRIUM FLOW FIELD SIMULATION

2.1 Mass, momentum and energy equations

In order to highlight gas vibrational nonequilibrium effects on radiative transfer, the plume is considered a single gaseous phase without metal oxide particles. This is the case, for instance, for rockets propelled with liquid fuels. Otherwise, particle radiation could become dominant. The flowing gas is a non-reacting mixture of CO_2-H_2O-CO-N_2 with other minor non-radiating species in the considered temperature range. The mixture corresponds to the experiment Titan IIIC described in Sec. 4. The flow field is calculated in the continuum approach using the Navier-Stokes equations with the multi-temperature formulation of vibrational disequilibrium. The continuum approach is shown to be a reasonable approximation for altitudes lower than typically 110 km [5] and is further justified by the fact that a significant part of the emitted radiation comes from the core of the plume, which is at relatively high pressure. Under these assumptions, the mass, momentum, and total energy balance equations write:

$$\partial_t\left(\rho_\mathrm{s}\right) + \partial_{x_j}\left(\rho_\mathrm{s} u_j\right) = \partial_{x_j}\left(\rho D_\mathrm{s} \partial_{x_j} Y_\mathrm{s}\right), \tag{1}$$

$$\partial_t\left(\rho u_i\right) + \partial_{x_j}\left(\rho u_i u_j\right) + \partial_{x_i} p = \partial_{x_j}\left[\mu\left(\partial_{x_j} u_i + \partial_{x_i} u_j\right) - \frac{2}{3}\mu \partial_{x_k} u_k \delta_{ij}\right], \tag{2}$$

$$\begin{aligned}\partial_t(\rho e_t) + \partial_{x_j}\left[(\rho e_t + p) u_j\right] = {} & \partial_{x_j}\left[\lambda_\mathrm{eq}\partial_{x_j} T + \sum_m \lambda_{\mathrm{vib},m}\partial_{x_j} T_{\mathrm{vib},m}\right] \\ & + \partial_{x_j}\left[\mu u_i\left(\partial_{x_j} u_i + \partial_{x_i} u_j\right) - \frac{2}{3}\mu u_i \partial_{x_k} u_k \delta_{ij}\right] \\ & + \partial_{x_j}\left[\rho \sum_{\mathrm{s}=1}^{N_\mathrm{s}} D_\mathrm{s}\left(e_{\mathrm{int,s}} + \frac{p_\mathrm{s}}{\rho_\mathrm{s}}\right)\partial_{x_j} Y_\mathrm{s}\right] + P^R\end{aligned} \tag{3}$$

where s is a given species, ρ_s and Y_s its density and mass fraction, D_s its mass diffusion coefficient, p_s its partial pressure, u_j the j^{th} component of the velocity. ρ and p designate the total density and pressure. The total energy per unit mass of the fluid e_t is the sum of kinetic and internal energy $e_t = e_\mathrm{kin} + e_\mathrm{int} = \frac{1}{2}u_j u_j + e_\mathrm{trans} + e_\mathrm{rot} + e_\mathrm{vib}$. For each vibration mode m of a given species s, the vibrational temperature $T_{vib,m}$ is determined from the vibrational energy balance equation:

$$\begin{aligned}\partial_t(\rho_\mathrm{s} e_{\mathrm{vib},m}) + \partial_{x_j}(\rho_\mathrm{s} e_{\mathrm{vib},m} u_j) = {} & \partial_{x_j}(\lambda_{\mathrm{vib},m}\partial_{x_j} T_{\mathrm{vib},m}) \\ & + \partial_{x_j}(\rho_s e_{\mathrm{vib},m} D_\mathrm{s}\partial_{x_j} Y_\mathrm{s}) \\ & + \Omega_m^{\mathrm{V-T}} + \Omega_m^{\mathrm{V-V}} + P_m^R,\end{aligned} \tag{4}$$

where $\Omega_m^{\mathrm{V-T}}$ and $\Omega_m^{\mathrm{V-V}}$ are the vibration-translation and vibration-vibration exchange terms. These terms are determined from a vibrationally detailed kinetic scheme as described in Ref. [3]. A specific scheme for HCl was also added to treat a more complex mixture. The total and partial radiative source terms, P^R and P_m^R respectively, will be detailed in Sec. 3. There are two vibrational temperatures for CO_2 (T_{12} and T_3) and one vibrational temperature for each diatomic molecule (T_CO, T_HCl and T_N2). H_2O is assumed at local thermodynamic equilibrium with the translation-rotation temperature T.

2.2 Transport properties and thermodynamics

The dynamic viscosity for each species μ_s was calculated according to Sutherland's laws. The mixture viscosity μ was then determined according to the formulation of Armaly and Sutton [6]. The thermal conductivity λ_{eq}, corresponding to the thermal conductivity of the energy modes at equilibrium (i.e. all the modes of the species at LTE and the rotational and translational modes of the species in vibrational disequilibrium), was computed from viscosities assuming a constant Prandtl number equal to 1 and using either the total specific heat capacities compiled by Capitelli et al. [7] (for species at LTE), or the trans-rotational specific heat capacities. The diffusion coefficients D_s were calculated with the ratio μ_s/ρ, assuming a constant Schmidt number equal to 1. Finally, the vibrational thermal conductivities $\lambda_{vib,m}$ were calculated according to Monchick et al. [8]. From a thermodynamic point of view, the vibrational heat capacities of NLTE species are represented by a harmonic oscillator model.

2.3 Numerical methods

The system of conservation equations was solved using a finite volume method with a general non-structured mesh. A second-order spatial reconstruction is performed using a multislope MUSCL method [9], and the Euler fluxes are calculated using an AUSM+ scheme [10], which was adapted to take into account the vibrational nonequilibrium. The time integration is performed using a first-order implicit method (implicit Euler) and a GMRES resolution. More details on the method of solution of the flow field in the framework of the multi-temperature model will be given in an extended version of the paper.

3. RADIATIVE TRANSFER AND SOURCE TERMS

Line by Line calculations in the framework of multi-temperature nonequilibrium flow were discussed in Binauld et al. [3] and were applied to the test case of the experiment BSUV-2. Due to CPU limitations, only a few lines of sight along the plume were considered to investigate the effects of CO_2 nonequilibrium radiation on the emitted intensity. In order to speed up the calculations and to enable coupled calculations with the flow field, a statistical narrow-band model was developed by Janodet et al. [4] for CO_2. This SNB model is extended here to CO_2-CO-HCl-H_2O mixtures. It is briefly described below, and its implementation in a Monte Carlo radiation solver is presented in Sec. 3.2.

3.1 The statistical norrow-band nonequilibrium model

We first assume that the absorption spectra of different molecules are statistically uncorrelated, so the mixture transmissivity can be computed as the product of individual transmissivities. At a high spectral resolution, the monochromatic intensity leaving a non-scattering gaseous column at abscissa s and wavenumber σ is given by:

$$I_\sigma(s) = I_\sigma(s_0)\tau_\sigma(s_0 \to s) + \int_{s_0}^{s} \frac{\eta_\sigma}{\kappa_\sigma}(s')\frac{\partial \tau_\sigma}{\partial s'}(s' \to s)\mathrm{d}s', \tag{5}$$

where η_σ and κ_σ are the emission and absorption coefficients, respectively, $\tau_\sigma(s' \to s)$ is the transmissivity between s' and s. The ratio $\frac{\eta_\sigma}{\kappa_\sigma}$ is equal to Planck's function when level populations follow the Boltzmann distribution at LTE. In order to build a SNB formulation from Eq. (5) by averaging over a narrow-band $\Delta\sigma$, the following uncorrelation hypothesis must be satisfied

$$\int_{s_0}^{s} \overline{\frac{\eta_\sigma}{\kappa_\sigma}(s')\frac{\partial \tau_\sigma}{\partial s'}(s' \to s)}^{\Delta\sigma} \mathrm{d}s' \approx \int_{s_0}^{s} \overline{\left(\frac{\eta_\sigma}{\kappa_\sigma}(s')\right)}^{\Delta\sigma} \frac{\partial \overline{\tau_\sigma}^{\Delta\sigma}}{\partial s'}(s' \to s)\mathrm{d}s'. \tag{6}$$

This is obviously the case at LTE since the Planck function is nearly constant inside $\Delta\sigma$. This assumption was also checked for diatomic molecules like CO and HCl [11]. However, due to the imbrication of several vibrational transitions in the same narrow-band, this approximation was not always valid for CO_2. This issue was solved in [4] by splitting the CO_2 spectroscopic database into three classes: the transitions with $\Delta v_3 = 1$, the transitions with $\Delta v_3 \neq 1$, and transitions for which the upper or lower vibrational level is not defined in HITEMP-2010. With this formalism, the intensity emitted by the gaseous column between s_0 and s is given by:

$$\overline{I}_{\sigma}^{\Delta\sigma}(s) = \sum_{j=1}^{N_{\text{contributor}}} \int_{s_0}^{s} \left[\overline{\left(\frac{\eta_\sigma}{\kappa_\sigma}\right)}_{j}^{\Delta\sigma}(s') \frac{\partial \overline{\tau_{\sigma,j}}^{\Delta\sigma}}{\partial s'}(s', s) \right] \prod_{j'\neq j} \overline{\tau_{\sigma,j'}}^{\Delta\sigma}(s', s)\, \mathrm{d}s', \tag{7}$$

where the contributors j to the radiation are here the classes ν_3, not-ν_3, and not-defined transitions of CO_2 molecule, and the transitions of the species HCl, CO and H_2O.

3.2 Implementation in a Monte Carlo radiation solver

The full coupling between flow field calculations and radiative transfer requires the computation of radiative source terms in total energy and vibrational energies balance equations. These source terms were calculated by implementing the SNB model in the Monte Carlo radiation solver ASTRE. Binauld et al. [12] have presented the implementation of the SNB model in ASTRE but under LTE assumption. We highlight here the main features of NLTE applications, and in particular, the calculation of the radiative source terms in the energy equations for each cell i of volume V_i:

$$P^R(i) = \frac{1}{V_i}(P_{\text{abs},i} - P_{\text{emi},i}) \quad \text{and} \quad P_m^R(i) = \frac{1}{V_i}(P_{\text{abs},i,m} - P_{\text{emi},i,m}) \tag{8}$$

where emitted powers $P_{\text{emi},i}$ and $P_{\text{emi},i,m}$ are calculated in a deterministic way such as:

$$P_{\text{emi},i} = 4\pi V_i \sum_{\text{band }\Delta\sigma} \sum_{j=1}^{N_{\text{contributor}}} \overline{\eta_{i,j}} \quad \text{and} \quad P_{\text{emi},i,m} = 4\pi V_i \sum_{\text{band }\Delta\sigma} \overline{\eta_{i,m}} \tag{9}$$

and absorbed powers $P_{\text{abs},i}$ and $P_{\text{abs},i,m}$ are performed using a Monte Carlo algorithm that simulates a large number of energy bundles following optical paths through mesh cells. Thus, for every cell i, the emitted power is divided into N_i energy bundles. Each bundle is randomly characterized by an emission point in the cell i and a direction, and associated with a contributor and a spectral band according to probability density functions. Then, each bundle leaves energy by absorption in every cell it passes through. In accordance with Eq. (7), absorption process can be written as:

$$P_{\text{abs},i} = \sum_{\text{cell } i'} P_{\text{abs},i}^{i'} = \sum_{\text{cell } i'} \sum_{j=1}^{N_{\text{contributor}}} P_{\text{abs},i}^{i',j} \tag{10}$$

where the absorbed power $P_{\text{abs},i}^{i',j}$ of a bundle emitted in a cell i' by the contributor j and absorbed in a cell i is given by the following expression:

$$\begin{aligned} P_{\text{abs},i}^{i',j} = \frac{P_{\text{emi},i',j}}{N_{i'}\overline{\kappa_{i',j}}\delta s} \Bigg[& \left(\overline{\tau_j}(s_{i'} + \delta s, s_i^-) - \overline{\tau_j}(s_{i'}, s_i^-)\right) \prod_{j'\neq j} \overline{\tau_{j'}}(s_{i'}, s_i^-) \\ & - \left(\overline{\tau_j}(s_{i'} + \delta s, s_i^+) - \overline{\tau_j}(s_{i'}, s_i^+)\right) \prod_{j'\neq j} \overline{\tau_{j'}}(s_{i'}, s_i^+) \Bigg] \end{aligned} \tag{11}$$

with $s_{i'}$, s_i^+, s_i^-, the abscissa respectively of the source point, the inlet and outlet points of the absorbing cell i, and δs a small column of length 10^{-6} m. In a similar way, the absorbed power $P_{\text{abs},i,m}$ is given by:

$$P_{\text{abs},i,m} = \sum_{\text{cell } i'} P^{i'}_{\text{abs},i,m} = \sum_{\text{cell } i'} \sum_{j=1}^{N_{\text{contributor}}} P^{i',j}_{\text{abs},i,m} \tag{12}$$

but, in this case, the absorbed power $P^{i',j}_{\text{abs},i,m}$ for each vibrational mode m could not be obtained directly and it is necessary to determine, beforehand, the absorbed power $P^{i',j}_{\text{abs},i,j'}$ by each contributor j' with the splitting formulation:

$$P^{i',j}_{\text{abs},i,j'} = P^{i',j}_{\text{abs},i} \frac{\widetilde{\kappa_{i,j'}}}{\sum_{j''=1}^{N_{\text{contributor}}} \widetilde{\kappa_{i,j''}}} \tag{13}$$

where $\widetilde{\kappa_{i,j'}}$ is the equivalent absorption coefficient of the j' contributor in the cell i. Afterwards, assuming that the absorbed power $P^{i',j}_{\text{abs},i,j'}$ is uncorrelated with the ratio $\overline{(\kappa_{i,\text{vib}}/\kappa_i)}_{j'}$, the power $P^{i',j}_{\text{abs},i,m}$ can be calculated as:

$$\begin{aligned} P^{i',j}_{\text{abs},i,m} &= P^{i',j}_{\text{abs},i,j'} \overline{\left(\frac{\kappa_{i,\text{vib}}}{\kappa_i}\right)}_{j'} \quad \text{for} \quad j' = \text{CO/HCl}, m = \nu_{\text{CO}}/\nu_{\text{HCl}} \\ P^{i',j}_{\text{abs},i,m} &= \sum_{\text{cl}=1}^{N_{\text{cl}}} P^{i',j}_{\text{abs},i,j'=\text{cl}} \overline{\left(\frac{\kappa_{i,\text{vib}_m}}{\kappa_i}\right)}_{\text{cl}} \quad \text{for} \quad m = \nu_{12}/\nu_3 \end{aligned} \tag{14}$$

where N_{cl} is the number of classes for CO_2 molecule. Note that the ratio $\overline{(\kappa_{i,\text{vib}}/\kappa_i)}_{j'}$ and $\overline{\eta_{i,m}}$ are additional model parameters calculated from the partial spectral absorption and emission coefficients defined in reference [3]. Validations of these formulations will be given in the case of 1D planar media in the extended version of the paper.

4. APPLICATION TO THE TEST CASE TITAN IIIC

4.1 Presentation of the experiment and simulation setup

This section is devoted to applying the developed models to the case of the experiment Titan carried out in the framework of programs MIDAS and TRIM in the sixties, as documented in Ref. [1]. We consider, in particular, the second stage of the rocket Titan IIIC flying at an altitude of 110 km and a velocity of 2905 m/s. The total length of the rocket is 19.68 m, and its diameter is 3.48 m [13, 14]. The gas mixture composition at the nozzle exit, in mass fractions, is N_2(0.412)-CO(0.0163)-CO_2(0.191)-N(0.00279)-O(0.00368)-NO(0.0175)-OH(0.00147)-H_2(0.00154)-H_2O(0.346)-O_2(0.00735)-H(0.00037), according to Ref.[1].
An iterative coupling between flow field calculations and radiative transfer is carried out until the results converge.

4.2 Comparison between results with different levels of radiation modelling

Figure 1 shows the vibrational temperatures of N_2 and CO with and without radiation. First, One can notice the plume's huge volume with a mixing layer between ambient external air and exhaust gases. While radiation effects on T_{N_2} are very weak, a strong cooling of several hundreds of Kelvins is observed for T_{CO} due to radiative losses. The same cooling effect is observed for CO_2 temperatures T_{12} and T_3 in Fig. 2. It is the most pronounced in the mixing layer region, which significantly contributes to plume radiation. These results demonstrate that, in the considered application, plume

signature cannot be predicted accurately by post-processing flow field calculations without coupling with radiative transfer.

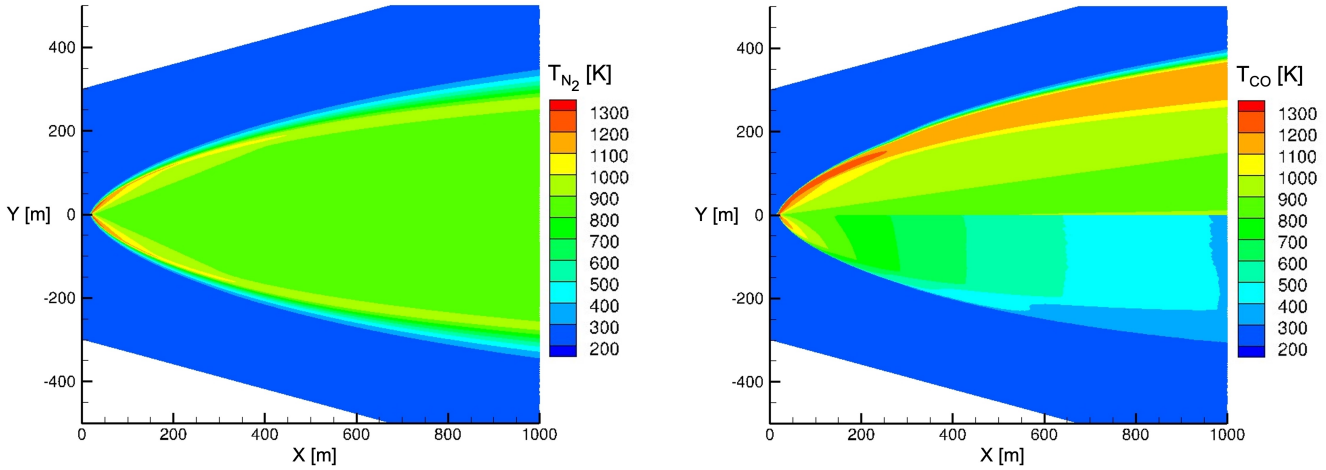

Figure 1: Comparison between N_2 (left) and CO (right) vibrational temperatures obtained from the coupled computation with radiation (Y<0) and without radiation (Y>0).

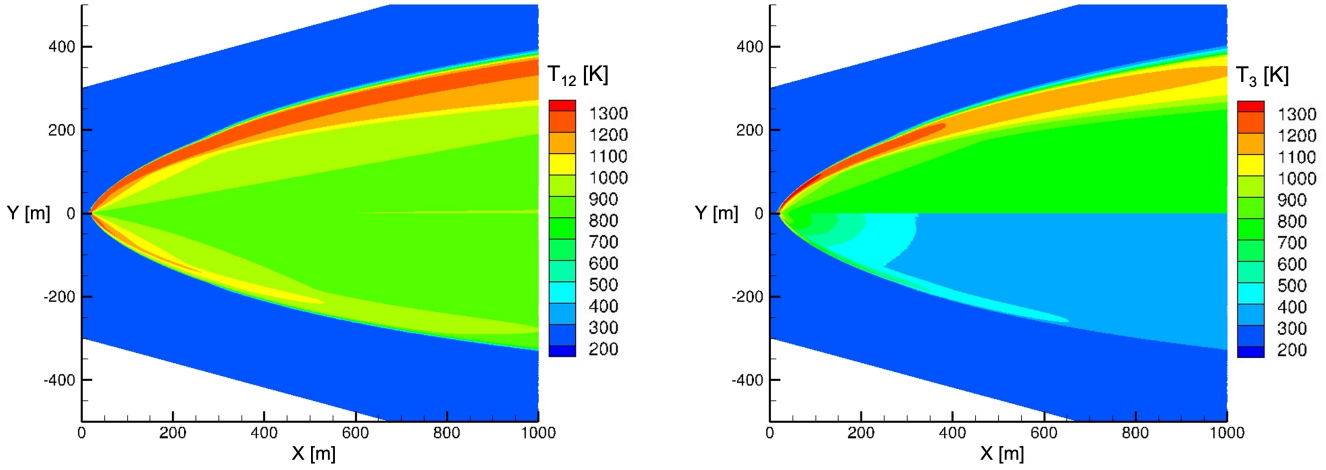

Figure 2: Comparison between CO_2 vibrational temperatures for modes ν_{12} (left) and ν_3 (right) obtained from the coupled computation with radiation (Y<0) and without radiation (Y>0).

Figure 3 shows the evolution of the various temperatures along the axis of the plume. Here, three levels of radiation modelling are considered: calculations without radiation, coupled calculations with optically thin radiation (only emission in the source terms), and fully coupled calculations considering absorption. First, one can notice that radiation does not significantly affect the translation/rotation temperature T, mainly governed by the thermodynamic expansion of the flow. All vibrational temperatures are significantly higher than T, regardless of the level of radiation modelling. The optically thin assumption leads to a strong decrease in vibration temperatures compared to the no-radiation case. However, absorption effects are shown to be important and tend to make vibrational temperatures closer to the no-radiation case, especially for CO_2 temperature T_3. The radiative source terms in the energy balance equations are shown in Figs. 4 and 5 for the total energy, CO_2 vibration mode ν_3, CO_2 vibration modes ν_{12}, and CO vibration mode. These source terms take significant values in the plume's core and the mixing layer region. Comparison between the source term in the total energy balance equation and the terms in the different vibrational energy equations show that most radiative losses are due to ν_3 vibrational energy exchange by radiative transitions.

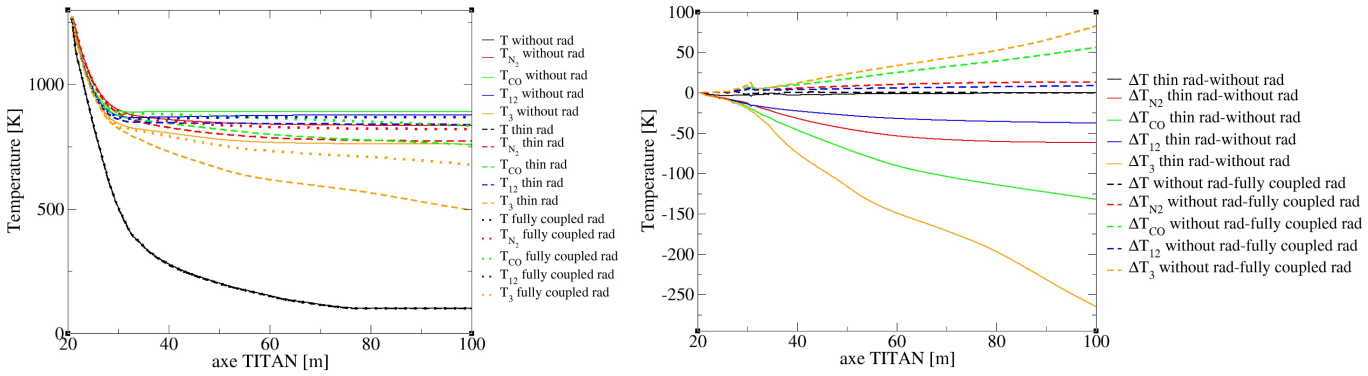

Figure 3: Evolution of the translation/rotation temperature and the vibrational temperatures along the plume axis. The compared profiles correspond to calculations without radiation, with optically thin radiation, and with the full coupling with radiative transfer. Differences are plotted on the right figure.

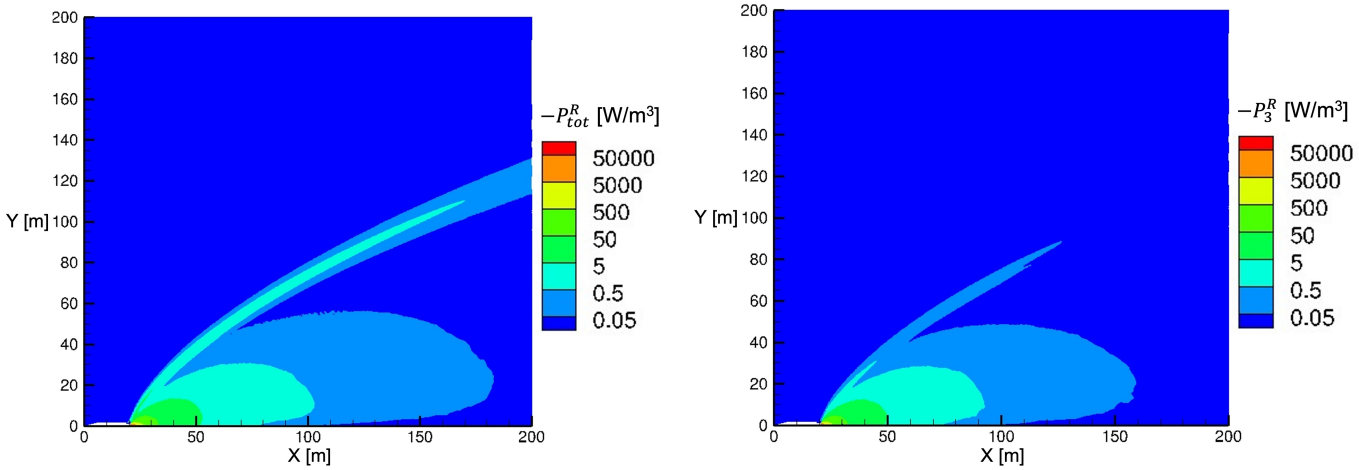

Figure 4: Opposite of the radiative source term (emission - absorption) in the total energy balance equation (left) and in the equation governing T_3 (right).

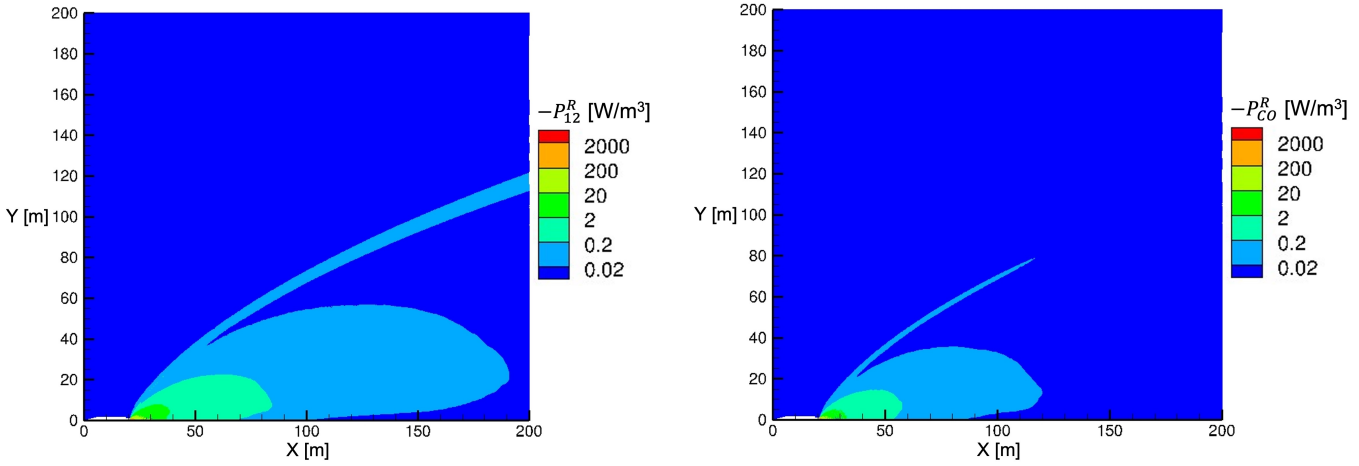

Figure 5: Opposite of the radiative source term (emission - absorption) in equation governing T_{12} (left) and T_{CO} (right).

5. CONCLUSION

A methodology for the prediction of coupled radiative transfer and non-equilibrium flow of high altitude rocket plumes was developed in this paper. Due to the impracticability of line by line

calculations and state to state description of the thermodynamic disequilibrium, a multi-temperature model was employed, and a statistical narrow-band model was developed for NLTE applications. This model was applied to test cases including CO_2-CO–HCl-H_2O-N_2 mixtures but could serve to predict several problems, including atmospheric entries. The developed SNB model was implemented in a Monte Carlo radiative transfer solver and coupled to a finite volume flow field code. The results showed that, in such applications, the radiative transfer has an important effect on both vibrational temperatures and the emitted radiation. Comparisons were made between uncoupled computations, computations with optically thin approximation, and computations including absorption in the plume. Results show that the coupling effects are really significant for predicting vibrational temperatures and plume radiation.

ACKNOWLEDGEMENT

The authors acknowledge the financial support of this study from the French Agence de l'Innovation de Défense, France (AID). This work was granted access to the HPC resources of IDRIS under the allocation 2022-A0102B00209 attributed by GENCI, France (Grand Equipement National de Calcul Intensif). This work was also performed using HPC resources from the Mésocentre computing center of CentraleSupélec and Ecole Normale Supérieure Paris-Saclay supported by CNRS, France and Région Ile-de-France, France (http://mesocentre.centralesupelec. fr/).

REFERENCES

[1] F. S. Simmons. *Rocket exhaust plume phenomenology.* Aerospace corporation, 2000.

[2] E. Nagnibeda and E. Kustova. *Non-Equilibrium Reacting Gas Flows.* Springer, 2009.

[3] Q Binauld, Ph. Rivière, J.-M. Lamet, L. Tessé, and A. Soufiani. CO_2 IR radiation modelling with a multi-temperature approach in flows under vibrational nonequilibrium. *Journal of Quantitative Spectroscopy and Radiative Transfer*, 239:106652, 2019.

[4] G. Janodet, Ph. Rivière, J.-M. Lamet, V. Rialland, L. Tessé, and A. Soufiani. Statistical Narrow Band model for vibrational nonequilibrium CO_2 radiation. *Journal of Quantitative Spectroscopy and Radiative Transfer*, 314(September 2023), 2024.

[5] Yu M. Kochetkov, A. M. Molchanov, and M. V. Siluyanova. Calculation of High-Altitude Jets of the Rocket Engine Based on Quasi-Gasdynamic Equations. *Russian Aeronautics*, 62(3):423–428, 2019.

[6] B. Armaly and K. Sutton. Thermal conductivity of partially ionized gas. *AIAA-81*, page 1174, 1981.

[7] M. Capitelli, G. Colonna, D. Giordano, L. Maraffa, A. Casalova, P. Minelli, D. Pagano, L. Pietanza, and F. Taccogna. Tables of Internal Partition Functions and Thermodynamic Properties of High- Temperature Mars-Atmosphere Species from 50 K to 50000 K. Technical Report STR-246, ESA, 2005.

[8] L. Monchick, A. Pekeira, and E. Mason. Heat conductivity of polyatomic and polar gases and gas mixtures. *The Journal of Chemical Physics*, 42:3241–3256, 1965.

[9] Clément Le Touze, Angelo Murrone, and Herve Guillard. Multislope MUSCL method for general unstructured meshes. *Journal of Computational Physics*, 284:389–418, 2015.

[10] Meng-Sing Liou. A sequel to AUSM: AUSM+. *Journal of computational Physics*, 129(2):364–382, 1996.

[11] G. Janodet, Ph. Rivière, J.-M. Lamet, V. Rialland, L. Tessé, and A. Soufiani. Modelling radiative properties of gas mixtures in nonequilibrium high-altitude rocket plumes. *Proceedings of the 10th International Symposium on Radiative Transfer, RAD-23*, pages 43–50, 2023.

[12] Q. Binauld, J.-M. Lamet, L. Tessé, Ph. Rivière, and A. Soufiani. Numerical simulation of radiation in high altitude solid propellant rocket plumes. *Acta Astronautica*, 158:351–360, 2019.

[13] William G. Purdy. Titan III core systems, integration and launch operations. *Journal of Spacecraft and Rockets*, 3(8):1177–1182, 1966.

[14] Marc Wade. Titan IIIC. *http://www.astronautix.com/t/titaniiic.html*, 2019.